THE POTENTIAL OF CROSS-POLARIZATION INFORMATION FOR OPERATIONAL SEA ICE MONITORING

B. Scheuchl [(1,,2)], **R. Caves** [(2)], **D. Flett** [(3)], **R. De Abreu** [(3)], **M. Arkett** [(3)], and **I. Cumming** [(1)]

[(1)]*Department of Electrical and Computer Engineering, University of British Columbia,*
2356 Main Mall, Vancouver, B.C., Canada V6T 1Z4

[(2)]*MacDonald Dettwiler and Associates,*
13800 Commerce Parkway, Richmond, B.C., Canada V6V 2J3

[(3)]*Canadian Ice Service,*
373 Sussex Drive, Ottawa, Ontario, Canada K1A 0H3

ABSTRACT / RESUME

The information content of ENVISAT ASAR alternating polarization data is evaluated with respect to operations at the Canadian Ice Service. A dual polarization data set covering an entire ice season is shown to have a higher information content compared to single polarization data. Automatic sea ice classification with dual polarization data is shown to have some potential to aid operational monitoring, but limitations due to system noise are noted.

1.   INTRODUCTION

RADARSAT-1, a spaceborne Synthetic Aperture Radar (SAR) with single polarization ScanSAR modes, is currently the primary data source for frequent, wide-area monitoring of sea ice, in particular for the Canadian Ice Service (CIS) [1]. Polarization diversity is expected to improve ice discrimination. Airborne polarimetric acquisitions since the late 80's (e.g. [2]) have proved useful for research, but have failed to address the seasonal aspect of ice signatures. The Advanced SAR instrument (ASAR) on the European Space Agency (ESA) ENVISAT satellite with its Alternating Polarization (AP) mode provides the first opportunity to investigate multi-polarization sea ice signatures over an entire ice season [3]. The 100 km AP swaths are too narrow for operational monitoring compared with ScanSAR, but ENVISAT ScanSAR does not offer multiple polarizations. However, ASAR AP data are very useful for application development in preparation for RADARSAT-2, which will provide dual polarization (HH+HV or VV+VH) ScanSAR data over 500 km swaths [4].

This paper reports first results of the analysis of ENVISAT ASAR AP data covering an entire season over an area in the Canadian Arctic near Resolute.

Table 1.   Data Availability

| Acqui-	ASAR Data		Aux. Data	
	Beam	*Pol.*	*Ice chart type*	*RADARSAT*
Apr. 3	IS6	HH+HV	Monthly	————
May 8	IS6	HH+HV	Weekly	May 6
June 12	IS6	HH+HV	Weekly	Same day
June 20	IS1	VH	Weekly	Same day
July 17	IS6	HH+HV	Weekly	Same day
July 25	IS1	VV+VH	Daily	July 24
July 27	IS5	VH	Daily	Same day
Aug. 3	IS3	VV+VH	Daily	Same day
Aug. 21	IS6	HH+HV	Daily	Same day
Aug. 31	IS5	HH+HV	Daily	Same day
Sept. 25	IS6	HH+HV	Weekly	N/A
Oct. 5	IS5	VV+VH	Daily	Same day
Oct. 18	IS4	VV+VH	Daily	Same day
Oct. 30	IS6	HH+HV	Weekly	Oct.31
Nov. 5	IS4	HH	Weekly	Nov.4
Nov. 9	IS5	VV+VH	Weekly	Same day
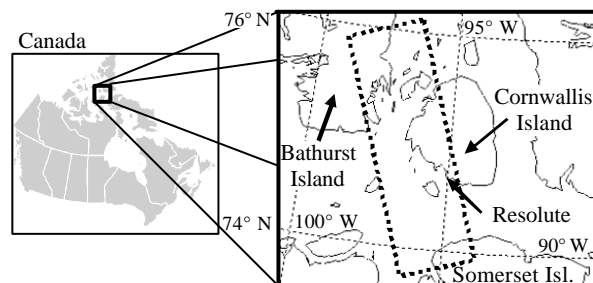
Figure 1.   Area of interest for ENVISAT ASAR AP data analysis. The IS6 APM swath coverage is shown by the dotted rectangle.

2. DESCRIPTION OF THE DATA SET

1.1. ASAR AP Data

Table 1 summarizes 16 ASAR AP data acquisitions between April and November 2003. During the sensor calibration phase ESA regularly acquired ASAR data over Resolute, one of the official calibration sites. Fig. 1 shows a sketch map of the area.

Table 2 shows the available swaths for ASAR AP data. Combinations of co- and cross-polarization data were collected over 13 passes (+ 3 single polarization scenes, see Table 1). RADARSAT-2 will provide these combinations for wide coverage ScanSAR modes, the mode of choice for CIS.

The medium resolution product (APM) was selected to approximate ScanSAR type resolution as well as to allow for longer acquisition lines. This product features a pixel spacing of 75 m and an equivalent number of looks (ENL) of approximately 50 [5].

1.2. Auxiliary Data

As part of their regular operation, CIS acquired RADARSAT-1 data and produced ice charts for the period in question (see Table 1). While RADARSAT-1 data represents the single most important information source used for ice chart production at CIS, other remote sensing data (e.g. NOAA AVHRR, SSM/I) are also utilized where available.

Mostly thick first year ice and old ice are identified in the region of interest. Several scenes contain areas of open water. Daily temperature (see Fig. 2), snowfall and wind data are also available.

The data set covers a wide range of environmental conditions. SAR acquisitions were made in both melting and freezing conditions (see Fig. 2). Calm wind (< 10 km/h) are reported for May 8, June 20, Aug. 3 and 31, Sept. 25, and Oct. 30. Wind speeds above 30 km/h are reported for April 3, Oct. 5 and 18, Nov. 5 and 9. Few significant snowfall events are reported, mostly in the fall with temperatures well below zero.

Table 2. ASAR Image Mode Swaths [5]

Swath	Swath with	Incidence angle range	Worst Case NESZ
-	km	[deg.]	[dB]
IS1	105	15.0 – 22.9	-20.4
IS2	105	19.2 – 26.7	-20.6
IS3	82	26.0 – 31.4	-20.6
IS4	84	31.0 – 36.3	-19.4
IS5	64	35.8 – 39.4	-20.2
IS6	70	39.1 – 42.8	-22.0
IS7	56	42.5 – 45.2	-21.9
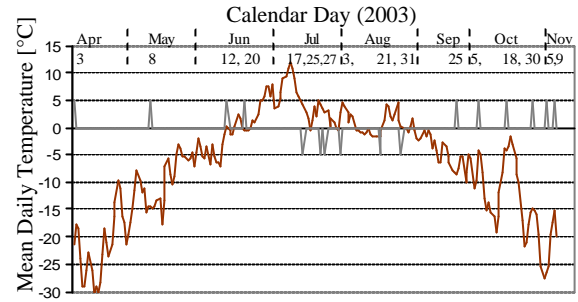
NESZ: Noise Equivalent Sigma Zero

Figure 2. Temperature record for Resolute with ASAR acquisition dates, the latter are shown in black.

3. DATA ANALYSIS

CIS operations are heavily based on human expert analysis. Data visualization is therefore an important aspect. In the analysis, the land area was masked out and the dynamic range of the HH and HV channels of the marine areas was evaluated.

Fig. 3 illustrates the difference in dynamic range for co- and cross polarization data. The histograms cover slightly different areas for different swaths, and a wide range of ice cover is represented. The examples show that for the data set at hand, the co-pol backscatter shows a dynamic range of about 14 dB, compared to approximately 8 dB for cross-polarized data. The sensor noise level restricts the lower limit of the dynamic range of the cross-polarization data.

VV data are shown to be on the higher end of the data interval, however, they were acquired at steep incidence or late in the season with a larger portion of brightly scattering deformed and old ice present in the area.

To ensure color consistency and allow visual comparison of the various scenes thresholds were applied to all scenes (see Fig. 3 for threshold values used). Examples for color and grey level representations of the data are shown in Fig. 4, 6, 7, and 8.

Cross sections across the swath in homogeneous areas (e.g., June 12, October 18) show a range variation of the cross-polarization component in homogeneous areas (see Fig. 4). As the cross-polarized channel is expected to have a small dependency on the incidence angle, little variation over the image swath should be present [3]. The observed variation is approximately 1.5 dB for IS6 First Year Ice (FYI) data and 4 dB for IS4 open water (data from other beams did not provide a homogeneous area over the full swath).

This variation in HV over the swath can be attributed to the variation of the signal/noise ratio (SNR). This noise limitation is not expected to be an issue for land applications. Low cross-polarized backscatter from smooth first year ice and open water compared to the noise level will affect both visual analysis and automated classification.
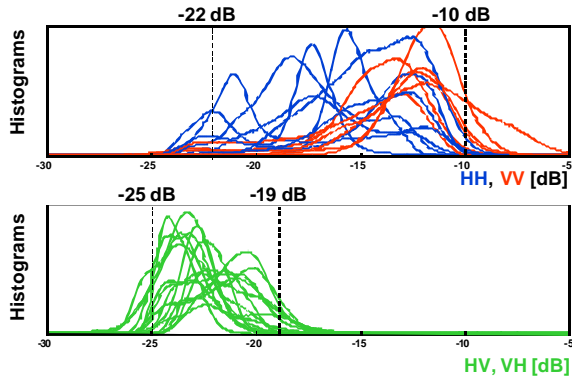
Figure 3. Dynamic ranges for marine areas for co- and cross-polarization backscatter. Histograms of different swaths cover different areas.
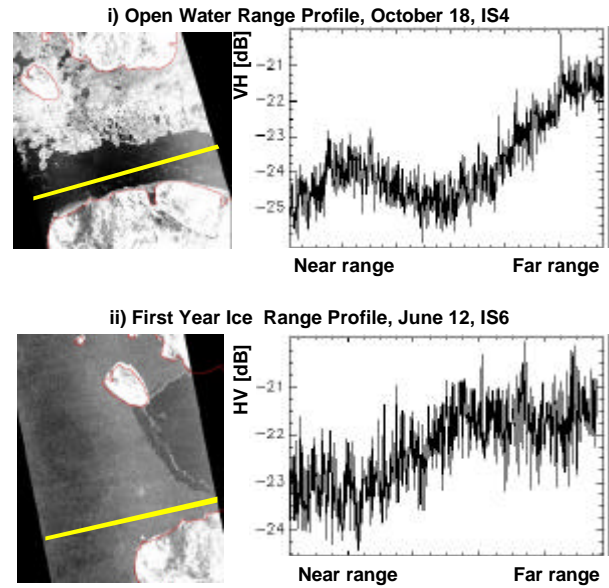

Figure 4. Range profiles for the cross-polarization channel. The two examples show system related variations of the signal level over homogeneous areas.

The top row of Fig. 8 shows all cross-polarized images acquired in beam IS6 (39.1° to 42.8° incidence angle). Old ice can easily be identified due to relatively high cross-polarized backscatter levels, except for images where wet snow obscures the signature (June 12, July 17).

The bottom row of Fig. 8 shows color images formed from the co- and cross-polarized channels. Representing both channels in a color image reveals the additional information content of alternating polarization data compared to single polarization data. Relative differences in co- and cross-polarization backscatter result in colors (blue for HV, and yellow for HH). Common attributes in both channels appear in grey levels (and white).

The April and May images (see Fig. 8) are very similar, with old ice present in the upper part of the images. Both scenes were acquired during stable, late winter ice conditions (though rising temperatures and 7.1 cm snow accumulation were observed). A more unified signature over the entire ice region can be observed for the June 12 image, associated with surface melt. Temperature data for the day confirm this assumption. The breakup of the ice can be seen in the July 17 image whereas in August, September and October the various stages of freeze-up are shown.

The change in ice type signatures over time is illustrated in Fig. 5, where the multi-temporal signatures of MYI and FYI are shown for the same region (see Fig. 8). The April 3, May 8 and June 12 scenes show stable ice conditions but significant variations in environmental conditions. The reduction in backscatter difference between the two ice types due to wet snow (June 12) is significant (>50%) for both channels. The backscatter levels between April and May are within 0.55 dB.
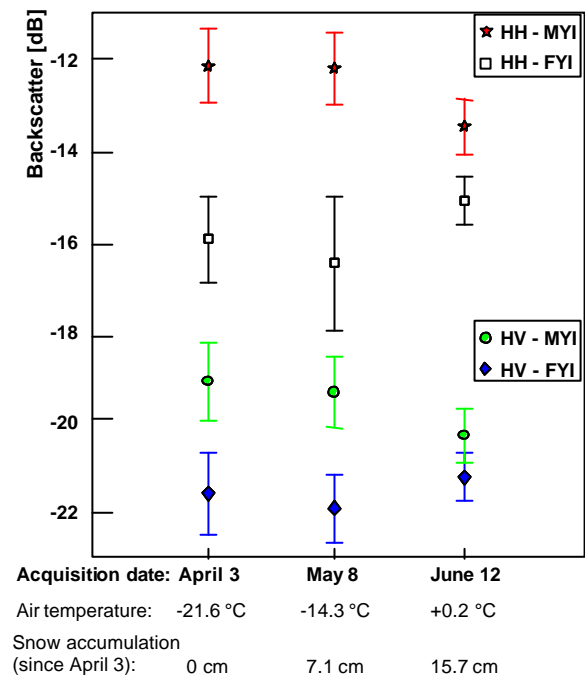

Figure 5. Multi temporal Multi Year Ice (MYI) and First Year Ice (FYI) signatures (+/- one standard deviation) for IS6 acquisitions. The MYI floe with surrounding FYI is indicated in Fig. 8.

4. CLASSIFICATION

A Canadian Ice Service ice chart indicates regions affected by sea ice and provides detailed information of the concentration of various ice types as well as the overall ice concentration. This information is indicated on charts using the WMO egg-code [6]. The charts are generated by ice analysts and/or ice forecasters, who make ice concentration and ice type estimates based on experience, information from previous charts as well as auxiliary information.

To date, automated algorithms using single polarization data have not proven accurate or consistent enough to be used in operations. While dual polarization data may not lead to fully automated systems in the near future, CIS has identified a number of areas where a classifier may aid an analyst. These are:

- Detection of old ice (embedded in first year ice)
- Ice vs. open water separation
- Detection of leads
- Ice concentration estimate

The latter three are closely related, as they require accurate separation of sea ice from open water. One additional challenge is the separation of smooth young ice and calm open water, as both tend to cause very low backscatter.

The Bayesian Wishart classifier has been shown to work for complex dual polarization data (i.e. partial scattering matrices) [7]. The authors also suggest an approach for detected dual polarization data, by modifying the distributions and using the magnitude of the channel correlation. In our study, we assume that the co- and cross-polarization channels are not correlated, and use the Wishart classifier with the detected dual polarization data.

Using this framework, the scalar distance measure d_2 is given as:

$$d_2 = \ln\left(|\mathbf{C_{2m}}|\right) + Trace\left(\mathbf{C_{2m}} \cdot \mathbf{Z}^{-1}\right)$$

where

$$\mathbf{C_{2m}} = E\left[\mathbf{Z} \mid w_m\right]$$

d_2 can be used efficiently for classification, where each pixel is assigned to the class with the minimum distance. Initial tests show promising results for ASAR AP data [4]. The matrix $\mathbf{C_{2m}}$ is the mean 2x2 reduced covariance matrix for class ω_m with zero off diagonal elements and $\mathbf{Z}$ is the 2x2 reduced covariance matrix of the pixel to be classified (also with zero off diagonal elements). E[ ] is the expected value.

The Wishart classifier is automatically initialized using four classes. The initial classes are set up by using the median values of the marine areas for the two channels to separate low and high backscatter pixels. The Bayesian classifier is run with three iterations, where the class means are updated after each iteration. Land areas are excluded from the classification by means of a land mask. The interpretation of the final classes is a manual task.

A reduction to two classes (ice and water) proved unsuccessful, as open water and sea ice areas were not successfully separated. This is likely because of the large variation of the ice signatures present, which is best accounted for by using more classes in the process.

All scenes with two polarizations available were classified using the method described. Table 3 provides a qualitative overview of the results.

Fig. 6 shows a color representation of both channels for September 25, 2003 (IS6, HH+HV), and a four-class classification result. The classification result preserves the spatial detail of the color image and groups together ice types with a common radar signature. However, it is not obvious if the blue class is open water or thin ice; these two scatterers cannot easily be separated.

Fig. 7 shows an color representation and a classification result for the July 25 scene, which was acquired in IS1 (VV+VH). The two images correspond well; the 4 class approach will be further investigated for its potential as semi automatic ice type concentration estimator (to aid ice analysts establishing egg codes for various regions). Note the generally low backscatter for thin ice (dark blue in classification result, black in the color representation) compared to low cross-pol and high co-pol backscatter for open water (light blue in classification result, bright yellow in the color representation).

For the IS6 scenes many classification results are are affected by the low level and the variation of the cross-polarization return over the swath. The April, May and June acquisitions show relatively stable ice conditions but environmental conditions change significantly. Table 4 shows confusion matrices evaluating the capability to classify MYI, the only class not affected by the HV variation. Between April and May, the classification performance is stable. Between April and June, a reduction in classification accuracy due to the wet snow layer and the resulting reduction in contrast can be observed. The rate of 67% MYI (April) classified as MYI (June) is underestimated partly due to a breakup of part of the ice in the June 12 scene (upper far range section in Fig. 8).

All other swaths show generally better classification results. Due to the limited number of scenes available per swath and different ice situations in the various scenes the result is not fully representative.

With the exception of the October 30 scene, performance issues can mostly be attributed to the low level of cross-polarization backscatter and to the system-related variation of the SNR over the swath. Further research is needed to address this issue, but ultimately, more power is required to get better results at higher incidence angles.
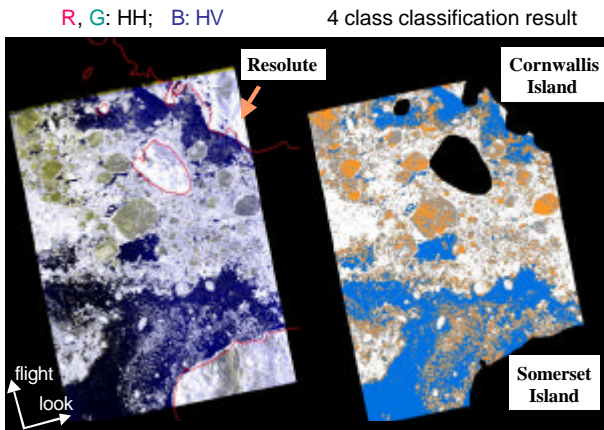
Figure 6.   Two-channel colour image (left) and clas-
sification result (right) of the Sep. 25 scene (IS6). The
color assignment for the right image is: white: deformed
ice, gray and orange: first year ice (slight differences in
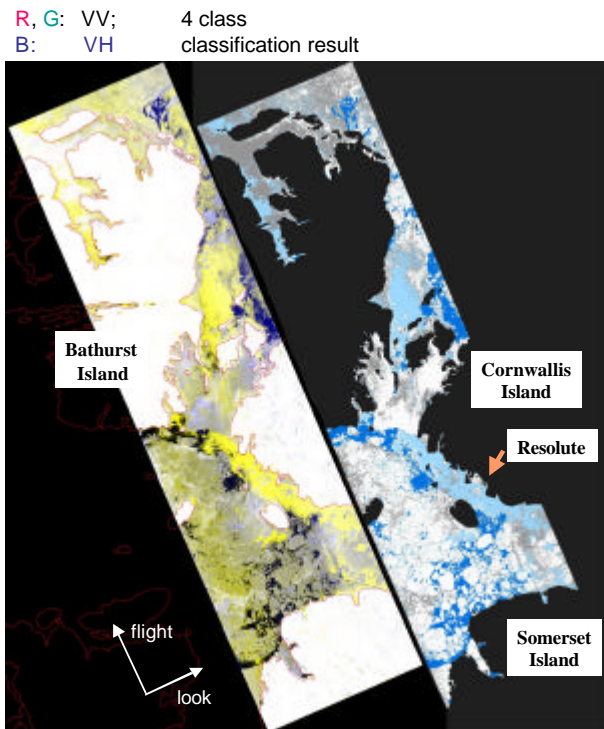roughness), blue: thin ice or possibly open water. Land
is shown in black.

Figure 7.   Two-channel colour image and classifica-
tion result (right) of the July 25 scene (IS1). The color
assignment for the right image is different from Fig. 5:
white, gray: first year ice (differences in roughness),
dark blue: thin ice, light blue: open water. Land is
shown in black.

Table 3.   Classification Evaluation (qualitative)

Swath	Scene	Performance criteria			
		Old ice de-tected	Ice vs. open water sepa-ration	Leads de-tected	Comment
IS6	Apr. 3	+	-	-	Inc. angle artifact
	May 8	+	-	-	Inc. angle artifact
	June 12	+	-	-	Inc. angle artifact + surface melt
	July 17	-	+	+	Surface melt
	Aug. 21	+	+	+	Large area of open water
	Sept. 25	N/A	+	N/A	Unsure if thin ice or open water
	Oct. 30	-	N/A	-	Overestima-tion of leads and MYI
IS5	Aug. 31	+	+	+	---
	Oct. 5	+	+	+	---
	Nov. 9	+	+	+	---
IS4	Oct. 18	+	+	+	Inc. angle artifact in far range
IS3	Aug. 3	N/A	+	+	---
IS1	Jul. 25	N/A	+	+	---

"+": Satisfactory result;   "-": Over- or under estimation of open water;
N/A: Not applicable for this scene

Table 4.   Multi temporal confusion matrices given
in % relative to the April scene. MYI only is compared
due to unsatisfactory classification performance for
other classes. See text for more detail.

IS6 acquisitions		April 3	
		MYI	Other
May 8	MYI	89	3
	Other	11	97
June 12	MYI	67	9
	Other	33	91

5. CONCLUSIONS

ENVISAT ASAR offers the first opportunity to study the utility of dual polarization sea ice data over one or more ice seasons. The higher information content tends to improve the estimation of the concentration of both the total ice content and the content of different ice types. The extra information can be conveniently visualized using color representations.

Semi-automatic information retrieval algorithms can be based on two SAR channels. Classification results were evaluated on the separation of sea ice and open water as well as the identification of old ice. Initial results are encouraging and should lead to tools that can help analysts with ice chart generation.

The use of spaceborne multi-polarization SAR data will be beneficial for operational sea ice monitoring in the future. While ASAR AP modes only provide limited spatial coverage, RADARSAT-2 will provide dual polarization ScanSAR data with a 500 km swath. SNR variations over the swath are shown to affect the classification and need to be addressed.

REFERENCES

1. Flett D., Operational use of SAR at the Canadian Ice Service: Present operations and a look into the future, in *Proceedings of the 2nd Workshop on Coastal and Marine Applications of SAR*, Svalbard, Norway , 8-12 September, 2003.

2. Drinkwater M.R., Kwok R., Winebrenner D.P., and Rignot E., Multifrequency polarimetric synthetic aperture radar observations of sea ice, *Journal of Geophysical Research*, 96(C11): 20,679-20,698, 1991.

3. Nghiem S.V., and Bertoia C., Study of multipolarization C-band backscatter signatures for Arctic sea ice mapping with future satellite SAR, *Canadian Journal of Remote Sensing*, vol. 27, no. 5, October, 2001.

4. Scheuchl B., Flett D., Caves R., and Cumming I., Potential of RADARSAT-2 data for operational sea ice monitoring, *Canadian Journal of Remote Sensing*, vol. 30, no.3, 2004.

5. European Space Agency (ESA), ENVISAT ASAR product handbook. ESA publication, Issue 1.1, December 2002.

6. Meteorological Service of Canada (MSC), MANICE – manual of standard procedures for observing and reporting ice conditions, Meteorological Service of Canada, Ottawa, Ont. 9th ed. April 2002.

7. Lee J.S., Grunes M.R., Pottier E., Quantitative comparison of classification capability: fully polarimetric versus dual and single-polarization SAR, *IEEE Transactions on Geoscience and Remote Sensing*, Volume: 39, Issue: 11, Pages: 2343 – 2351, Nov. 2001.
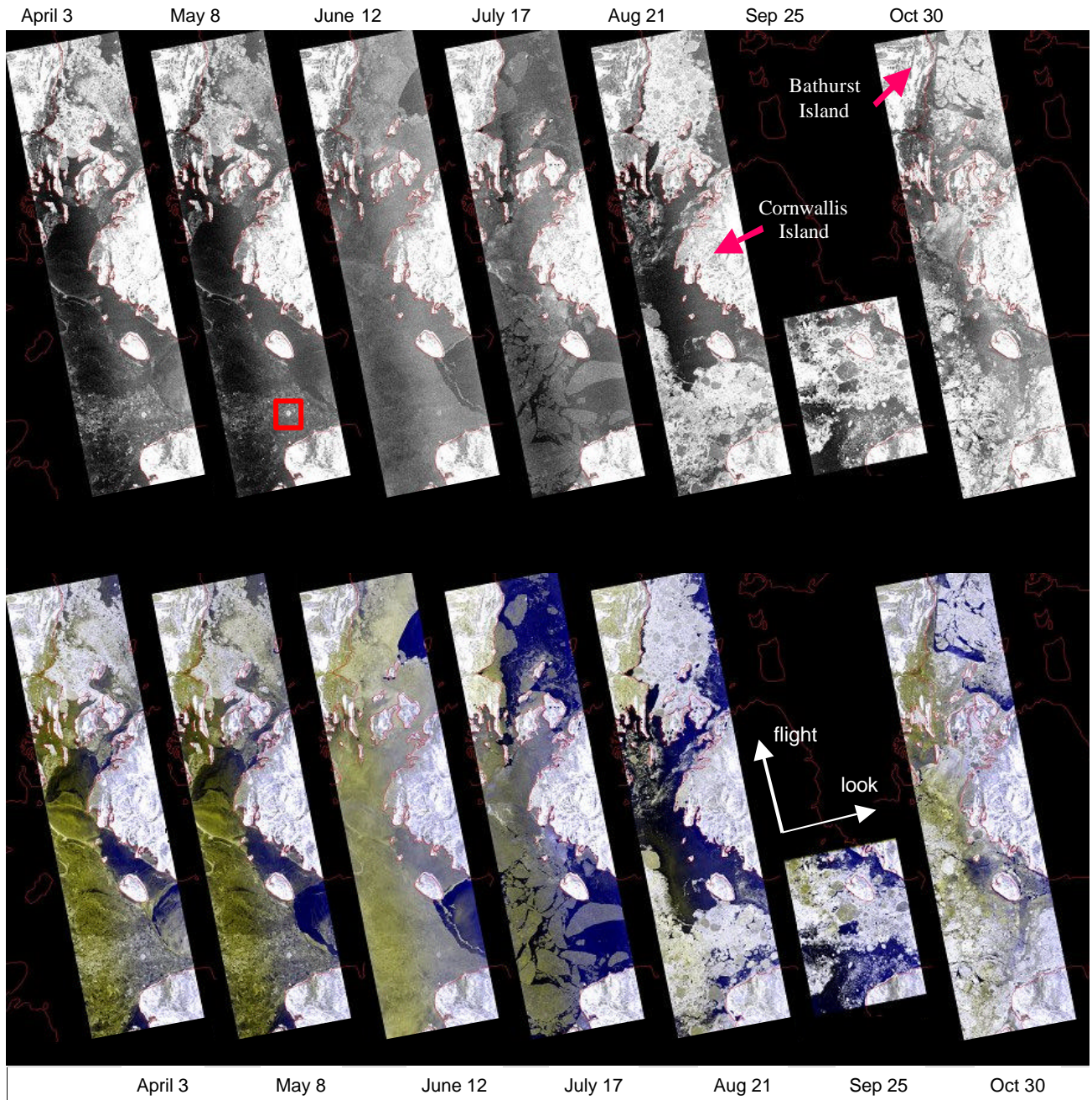
Figure 8.   ASAR APM IS6 images acquired in 2003. Top row: HV scaled from -25 dB to -19 dB. Bottom row: R,G (yellow): HH scaled from -22 dB to -10 dB; B: HV (scaled as above). Old or compressed ice shows as bright grey, open water or thin ice shows in blue. Note the variation of HV over the swath in the upper row (especially in the early season images), which creates a yellow band in the color images below, adversely affecting the interpretation. The red rectangle shown in the upper row indicates an MYI floe embedded in FYI. A backscatter analysis of this region for the April, May, and June scenes is shown in Figure 5.